IEEE Journal of Microwaves

Received 5 April 2023; accepted 1 June 2023. Date of publication 22 June 2023; date of current version 7 July 2023.

Digital Object Identifier 10.1109/JMW.2023.3283152

Estimation of the Effects of Spurious Modes in Linear Microwave Systems Using a Monte Carlo Algorithm

BURKHARD PLAUM

Institute for Interfacial Process Engineering and Plasma Technology, University of Stuttgart, 70569 Stuttgart, Germany
(e-mail: burkhard.plaum@igvp.uni-stuttgart.de)

This work was supported by the Max Planck Institute for Plasma Physics, Garching and Greifswald, Germany

ABSTRACT The effects of spurious modes on the performance of microwave systems is studied using a Monte Carlo algorithm based on randomized mode mixtures. A high power microwave launcher for the heating of fusion plasmas is used as an example, but the method can be applied to arbitrary linear optical systems. The linearity allows to simulate the beam propagation only for the pure modes while the actual Monte Carlo analysis is done using linear combinations of these fundamental solutions. This significantly decreases the calculation time. The results are histograms for truncation losses on mirrors, peak power densities and the overall efficiency. These results allow the definition of safety margins when designing high power millimeter wave components. In addition, a worst-case prediction for reduction of the overall efficiency due to spurious modes can be confirmed by the Monte Carlo analysis.

INDEX TERMS ECRH, Monte Carlo, plasma heating, spurious Modes.

I. INTRODUCTION

In high-power millimeter-wave systems for thermonuclear fusion experiments using corrugated waveguides with the LP_{01} (aka HE_{11}) mode, the effects of spurious modes (also called higher-order modes or HOMs) become increasingly important due to the high powers and increased pulse lengths in experiments like ITER or Demo. Sources of HOMs include:

- Non-perfect coupling of the gyrotron beam into the waveguide
- Manufacturing and assembly tolerances of transmission line components (e.g. waveguides or mirrors)
- Bending of waveguides due to thermal expansion or gravitational sag
- Diffraction by miter bends

HOMs can have many unwanted effects, which are, among others:

- Higher local fields, which can cause overheating on mirrors or arcing near vacuum windows
- Increased truncation losses at mirrors due to the larger beam divergence
- Non-optimal beam parameters in the plasma resulting in a decreased heating efficiency
- Spurious beam lobes going in unwanted directions, where they can damage sensitive in-vessel components

Very high order modes have a strong attenuation and usually disappear after a few meters resulting in higher heat loads in the waveguide walls. Low order HOMs, which are the main subject of this study, can propagate over longer distances and affect the fields in the launcher.

To study the change of the Gaussian beam parameters due to HOMs, there are two possible approaches: Either the total field is calculated at the locations of interest and the modified Gaussian parameters are obtained with a fit procedure. The alternative approach is to define the nominal (i.e. without HOMs) Gaussian beam as the fundamental mode and all deviations as higher order Gaussian modes. The second approach is less intuitive but simpler and faster because the analysis methods presented here work for Gaussian modes as well as for waveguide modes.

The elementary mechanisms of HOM generation have been studied for decades ([1], [2], [3], [4], [5], [6]) and are well understood and verified experimentally. The overall HOM spectrum at the end of a transmission line is, however, difficult to predict because the types and locations of the imperfections are obviously not known in advance. Furthermore, multiple sources of HOMs are subject to interference, which can be constructive or destructive. In addition, the HOM generation is time dependent on different scales (e.g. due to thermal

expansion or relative movement of buildings). This makes the HOM generation itself a natural candidate for Monte Carlo methods [7].

This study focuses on the effects of HOMs on the performance of an ECRH launcher, where random HOM mixtures are generated and the effects are analyzed with a Monte Carlo method. To simplify our analysis and increase the calculation speed, we utilize fundamental properties of linear systems, most notably the superposition principle.

It is worth noting, that this study is meant as a *risk assessment* mainly for determining the robustness of a design with respect to HOMs and for defining safety margins or maximum power levels. Therefore it would be extremely difficult to verify the results experimentally since it would require the generation of randomized mode mixtures and thousands of measurements.

The paper is organized as follows: In Section II we summarize the well known linearity principle and its implications for the analysis of electrical circuits and optical systems. Section III describes the simple generator for randomized mode mixtures, which was used in this study. In Section IV we introduce a hypothetical ECRH launcher and describe the calculation methods used for the simulation. The results from the Monte Carlo analysis are presented in Section V followed by the conclusions (Section VI) and outlook (Section VII).

II. LINEAR SYSTEMS

Generally speaking, a physical system is considered linear with respect to a signal $S(\omega)$, if the complex transfer function $H(S, \omega)$ can be written as:

$$H(S, \omega) = S(\omega) \cdot h(\omega) \tag{1}$$

where $h(\omega)$ represents the behavior of the system. From this formulation in the frequency domain we can easily derive the superposition principle, which can be written as:

$$H[S_1(\omega) + S_2(\omega)] = H[S_1(\omega)] + H[S_2(\omega)] \tag{2}$$

The superposition principle implies, that the behavior of the system with respect to the signal S_1 is not affected by the presence of a signal S_2 in the same system.

All electromagnetic systems are linear with respect to the electric and magnetic fields as long as the material properties (σ, ϵ and μ) are independent of the field amplitudes. For high power microwave systems consisting only of passive components, this is the case as long as no arcing occurs.

Linearity plays an important role for the analysis of complex electrical networks with multiple input- and output ports, where matrix formalisms have been used for several decades to fully describe their behavior [8]. In optical or waveguide based systems, equivalent formalisms can be used, where the different input- and output ports correspond to different field modes [9].

Fig. 1 illustrates this equivalence. For the electrical circuit (left), the vector $\vec{U_o}(\omega)$ of the output voltages can be obtained from the input voltages $\vec{U_i}(\omega)$ by a matrix multiplication:

$$\vec{U_o} = (M)_{el}\vec{U_i} \tag{3}$$

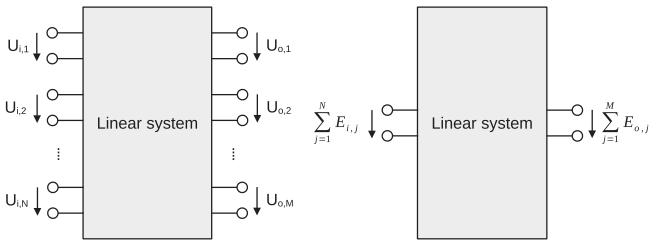

FIGURE 1. Equivalence of a discrete electrical multi-port network (left) and an optical multi-mode system (right).

while for an optical or a waveguide system, the equation for the field strengths becomes:

$$\vec{E_o} = (M)_{opt}\vec{E_i} \tag{4}$$

In practice, the most commonly used matrix formalism is the scattering matrix. The basic principles discussed here are, however, independent from the actual formalism.

From these considerations, we can formulate two hypotheses, which can be proven theoretically from the linearity principle and will both be validated in Section V.

The first hypothesis states that for a Monte Carlo simulation of a system with thousands of mode mixtures, it is sufficient to solve the problem for the pure modes, which are involved. If the field values for these fundamental solutions are saved in terms of complex electric (or magnetic) field vectors at the locations of interest, the solutions for arbitrary mixtures can be obtained by simply calculating the linear combination of these fundamental solutions. The background of this hypothesis is, that the number of dominant modes is usually quite small (< 10) but the solver used to simulate e.g. the reflection on a mirror can take several hours to complete. The calculation of the linear combination of the fields, however, is a matter of a few seconds. In this study, which used 10000 mixtures with 8 modes involved, this allowed us reduce the total calculation time by about 3 orders a magnitude.

The second hypothesis provides a *worst-case* estimation for the overall efficiency as a result of HOMs. Whenever the efficiency of a system is defined in terms of a global power ratio, the worst possible impact of X percent spurious modes is a reduction of this efficiency by X percent. The explanation is based on the superposition principle (2): X percent of HOMs mean (100-X) percent of the power in the main mode. And from the superposition principle we know that the propagation of the main mode is not affected by the HOMs. The worst-case would occur, if the power in the HOMs would be completely lost, which is usually not the case. This estimation is valid only for a global energy balance over a larger cross-section. It cannot predict local effects, which are dominated by interference and can only be assessed statistically.

III. GENERATION OF THE MODE MIXTURES

For the present study we used a very simple generator, which assumes that the probability distribution of the power is identical for all HOMs involved. See Section VII for possible

approaches to generate more realistic mode mixtures. For every HOM m in every mixture n, the initial (unnormalized) amplitude $\tilde{A}_m^n$ is calculated as:

$$\tilde{A}_m^n = \sqrt{r_1} e^{j2\pi r_2} \tag{5}$$

where r_1 and r_2 are uniformly distributed random numbers between 0 and 1. This implies that the power and the phase of the modes are uniformly distributed.

In order to get a defined total power percentage of HOMs, we first need to normalize the total HOM power to unity:

$$A_m^n = \frac{\tilde{A}_m^n}{\sqrt{\sum_{m=1}^{M} |\tilde{A}_m^n|^2}} \tag{6}$$

where M is the total number of HOMs. The total field of a mixture n with a defined relative HOM power p_H is then obtained with:

$$\vec{E}_{n,p_H} = \sqrt{1-p_H} \cdot \vec{E}_{\mathrm{LP}_{01}} + \sqrt{p_H} \left(\sum_{m=1}^{M} A_m^n \vec{E}_m \right) \tag{7}$$

where $\vec{E}_{\mathrm{LP}_{01}}$ is the field of the LP_{01} mode and $\vec{E}_m$ is the field of the mode m. Both $\vec{E}_{\mathrm{LP}_{01}}$ and $\vec{E}_m$ need to be normalized for unity power.

For the present study we used 10000 mixtures. The HOM power levels are 5% and 10% respectively, where the latter is higher than the levels, which are usually expected in ECRH systems. Fig. 2 shows the resulting distributions of the frequency of occurrence for the power and phase of the LP_{02} mode. The power distribution is no longer uniform because of the normalization according to (6). The distributions of the other HOMs are equivalent because the mixture generator does not distinguish between them.

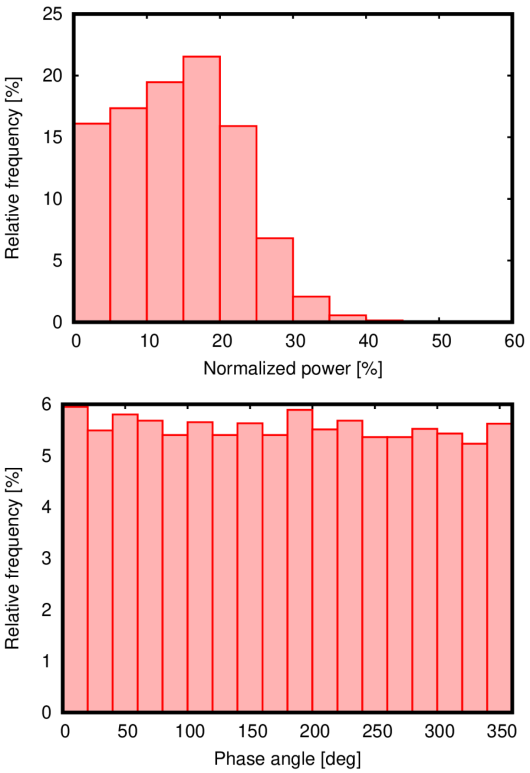

FIGURE 2. Distribution of the power (top) and phase (bottom) of the LP_{02} mode after normalization according to (6).

IV. EXAMPLE

As an example we choose a hypothetical ECRH launcher, which is fed by a corrugated waveguide with the LP_{01} as the main mode. The waveguide diameter is 50 mm, the frequency is 170 GHz. The launcher consists of a focusing mirror (focal length: 1.5 m) with a limited size, which directs the beam to a location in the plasma (see Fig. 3). The mirror size was chosen such that it captures most of the beam power (99.77 %) for the case of a pure LP_{01}-mode.

For the calculation of the mirror reflection we use the Physical Optics solver from the PROFUSION code package [10], which was already successfully used in previous studies [11]. The field from the waveguide is propagated by an FFT-based plane wave decomposition to different distances in order to obtain a 3D interpolation grid for the electric field. Together with the local k-vectors (derived from the gradient of the phase angle of the electric field) and the free-space impedance the magnetic field vector can be obtained at arbitrary locations. The mirror surface is discretized using a Cartesian grid with a spacing smaller than $\lambda/2$. On each of the surface elements the induced current $\vec{J}$ is calculated from the incident

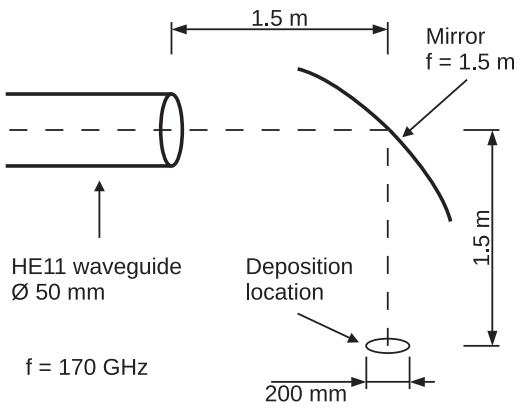

FIGURE 3. Example launcher.

magnetic field $\vec{H}_i$ with

$$\vec{J} = 2\vec{n} \times \vec{H}_i \tag{8}$$

where $\vec{n}$ is the outward pointing normal vector on the mirror surface. From the current, the radiated magnetic field can be calculated using the Green function of free space:

$$\vec{H}_r = \iint \left(-jk - \frac{1}{R} \right) \cdot \vec{J} \times \frac{\vec{R}}{R} \frac{e^{-jkR}}{4\pi R} dydx \tag{9}$$

Here, $\vec{R}$ is the vector from the point on the mirror to the location, where $\vec{H}_r$ is calculated. The calculation of the reflected field pattern on a rectangular area results in 4 nested loops.

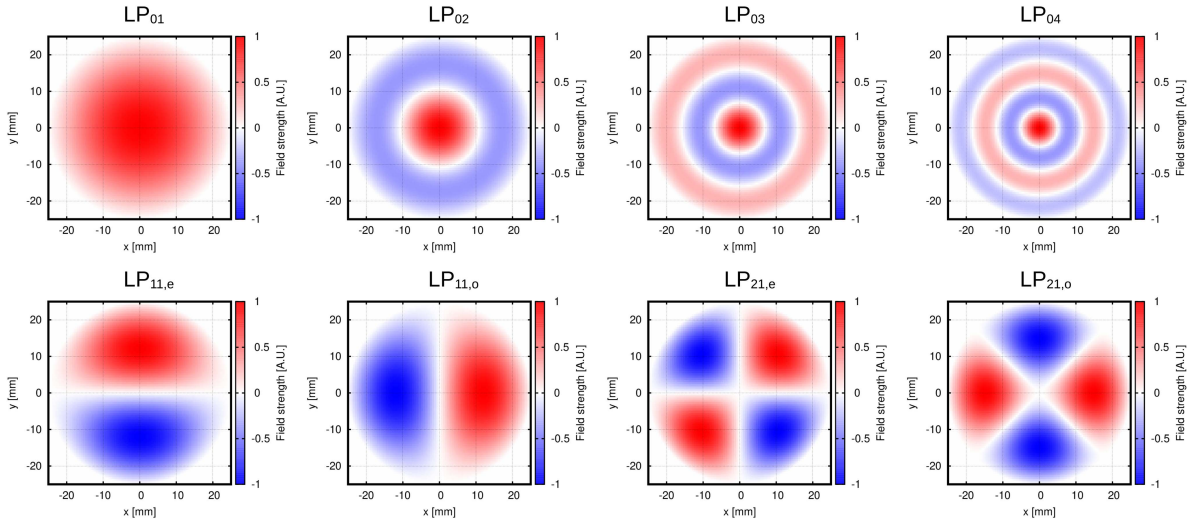

FIGURE 4. **Modes used for the simulation.**

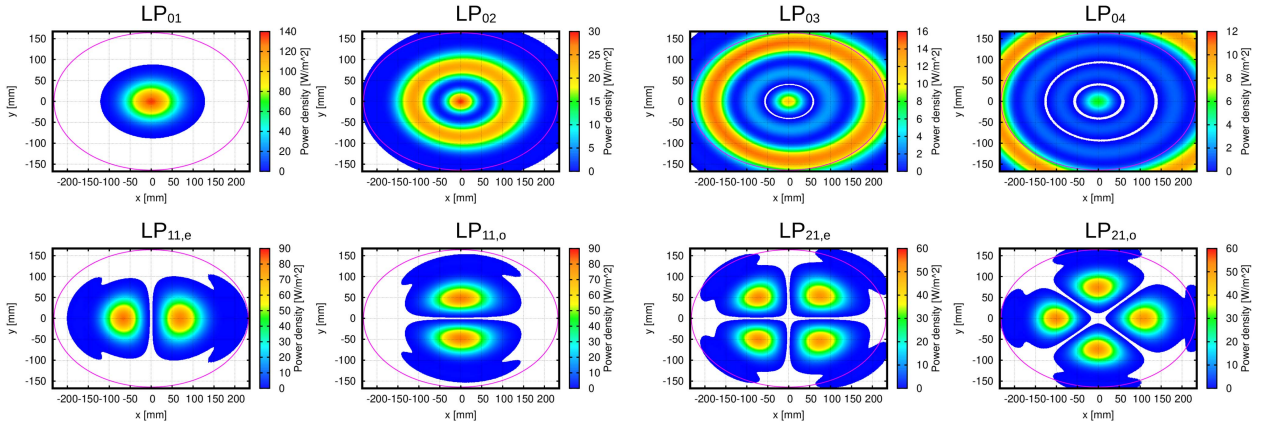

FIGURE 5. **Incident fields on the mirror for the pure modes. The ellipse denotes the mirror boundary.**

The outermost loop is therefore parallelized to run on different CPU cores.

After the mirror we assume a circular deposition area in the plasma, which has a diameter of 200 mm. The total efficiency of the system is defined by the total power, which is inside of this area.

At the waveguide aperture, the field is given in terms of linearly polarized LP_{mn} modes, which are commonly used when modeling transmission lines consisting of corrugated waveguides [12]. The modes, which were taken into account for this study, are shown on Fig. 4. The fundamental mode is the LP_{01}. The LP_{02}, LP_{03} and LP_{04} are excited, if the diameter of the free space beam is not perfectly matched to the waveguide radius when the beam is coupled into the waveguide or by waveguide gaps. The $LP_{11,e}$ and $LP_{11,o}$ represent a slight shift or tilt of the beam axis, while the $LP_{21,e}$ and $LP_{21,o}$ represent an elliptical deformation of the field pattern.

The system was simulated for the pure modes and the fields of the fundamental solutions were saved as 2D distributions on the surface of the mirror and in the plane of the deposition area. Then, the linear combinations according to the mixtures were calculated with (7) on order to obtain the following parameters:

- The truncation loss of the mirror (i.e. the power outside of the boundary curve)
- The peak power density on the mirror
- The total power inside of the deposition area

V. RESULTS

A. FUNDAMENTAL SOLUTIONS

To investigate the possible effects of the single HOMs, the fundamental solutions are summarized here. The power density of the incident fields on the mirror is shown in Fig. 5 for pure modes coming from the waveguide, assuming a total power at the waveguide aperture of 1 W. The ellipses denote the mirror boundary. We can see that the the basic symmetry properties of the modes are preserved and that the increased divergence of the higher order modes causes a significant portion of the power to be outside of the mirror. The

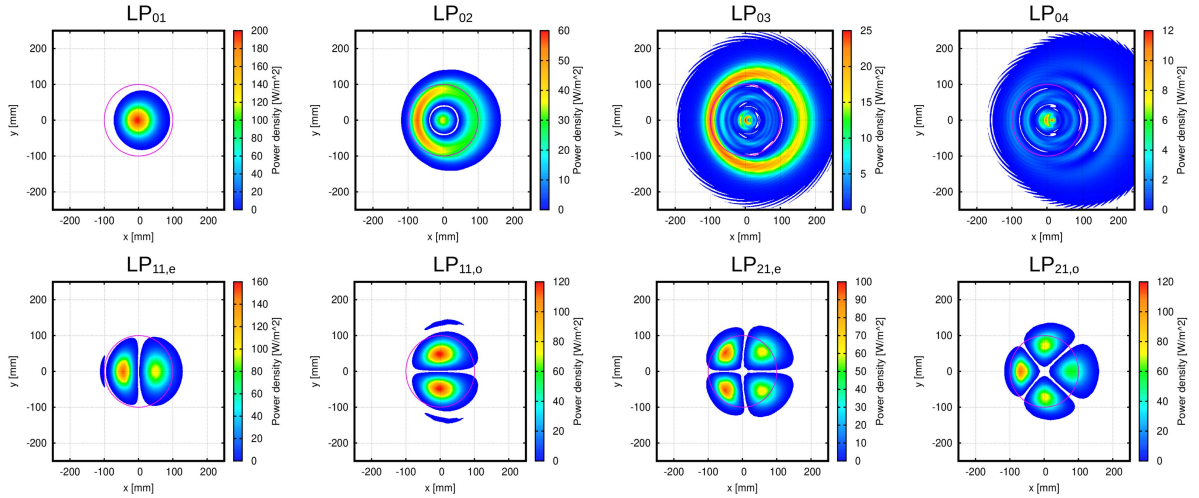

FIGURE 6. Fields in the deposition plane for the pure modes. The circle denotes the boundary of the deposition area.

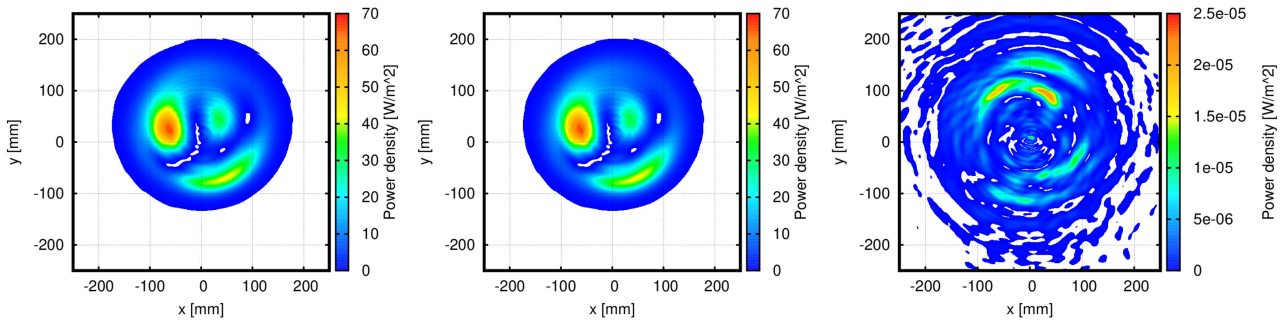

FIGURE 7. Field at the deposition plane calculated by propagating the mixture through the systems (left) and by adding the fundamental solutions (center). The difference of the results is shown in the right plot. Note the different scales.

TABLE 1 Truncation Losses for the Fundamental Solutions

Mode	Truncation loss [%]
LP_{01}	0.23
LP_{02}	1.85
LP_{03}	19.77
LP_{04}	87.94
$LP_{11,e}$	0.63
$LP_{11,o}$	0.51
$LP_{21,e}$	1.48
$LP_{21,o}$	1.47

TABLE 2 Power in the Deposition Area for the Fundamental Solutions Normalized to the Power in the Waveguide

Mode	Power [%]
LP_{01}	99.19
LP_{02}	71.66
LP_{03}	12.41
LP_{04}	3.55
$LP_{11,e}$	95.72
$LP_{11,o}$	96.91
$LP_{21,e}$	80.45
$LP_{21,o}$	80.17

additional beam lobes for the LP_{11}- and LP_{21}-modes are due to diffraction by the waveguide boundary and can also be seen if the fields of these modes are propagating in free space.

Table 1 shows the values for the truncation losses. From Fig. 5 and Table 1 we can conclude that in this example the most critical HOMs in terms of increased beam divergence and mirror truncation are higher order LP_{0m} modes.

The fields in the deposition plane for the pure modes are shown in Fig. 6. Here the circle denotes deposition area, over which the plasma power is integrated for obtaining the total efficiency. We can see a slight asymmetric deformation, which occurs due to the non-perpendicular incidence of an expanding beam on a curved mirror as discussed in detail e.g. in [13], [14] and [15]. The total power in the deposition area is summarized in Table 2.

B. VALIDATION OF THE METHOD

To verify the framework and especially the first hypothesis from Section II the power in the deposition plane was calculated for one mode mixture with two methods. First the

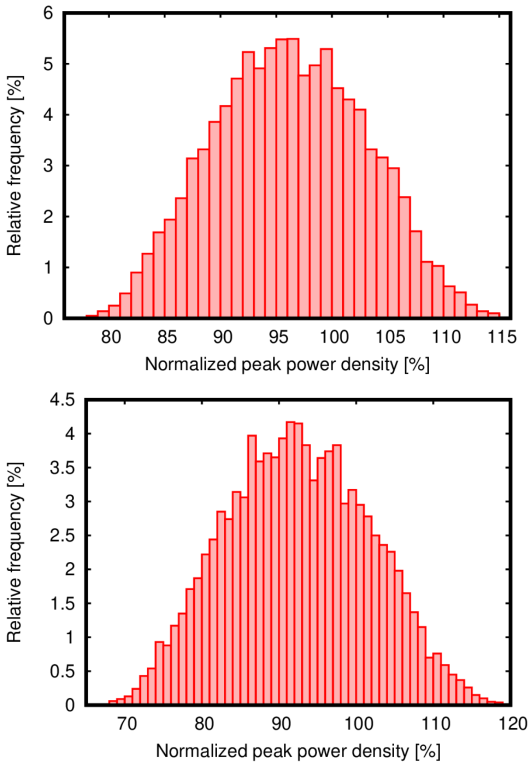

FIGURE 8. Normalized peak power on the mirror for a HOM power of 5% (top) and 10% (bottom). 100% peak power correspond to a pure LP_{01} mode.

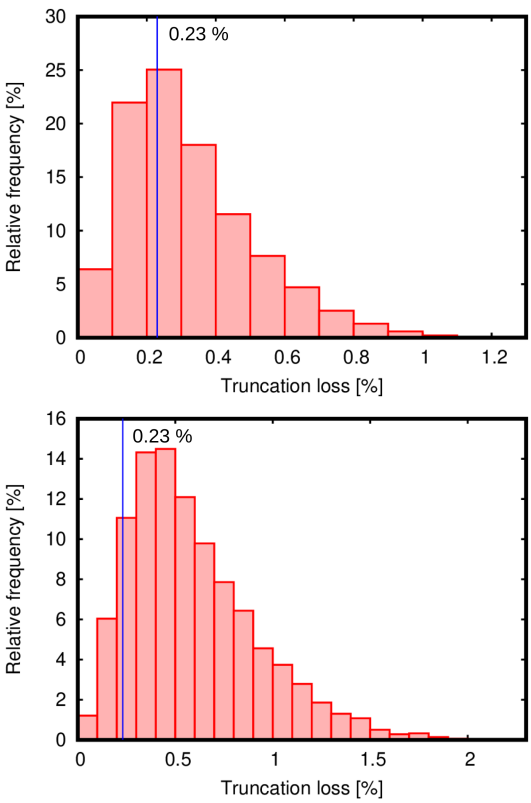

FIGURE 9. Truncation loss of the mirror for a HOM power of 5% (top) and 10% (bottom). For a pure LP_{01} mode the loss is 0.23% denoted by the blue line.

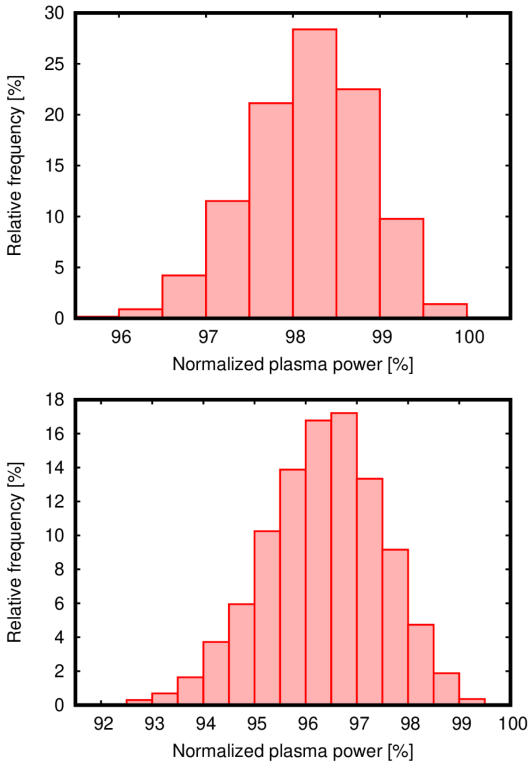

FIGURE 10. Power in the deposition area for a HOM power of 5% (top) and 10% (bottom). 100% power correspond to a pure LP_{01} mode.

mixture was generated at the waveguide aperture and propagated through the system to the deposition plane. In the second calculation, a linear combination of the fundamental solutions in the deposition plane (see Fig. 6) was calculated using the same mixing factors as for the first method. To verify that the method works even for extreme cases, the LP_{01} content is zero in this example. The results are shown in Fig. 7. The left and center images show the field in the deposition plane for the first and second case respectively. The images look practically identical. The difference between the solutions is shown in the right plot. The relative power of the difference signal is -47 dB and therefore negligible.

C. EVALUATION OF THE RESULTS

For estimating the impact of HOMs on the system performance, the fundamental solutions on the mirror (Fig. 5) and in the deposition plane (Fig. 6) were used to calculate the total fields for 10000 mixtures according to (7). The peak power density and the truncation loss on the mirror as well as the total power in the deposition location were calculated for each of the mixtures for total HOM-powers of 5% and 10%. The results for the peak field on the mirror are shown in Fig. 8. From these histograms we can conclude, that for this particular example, the peak power density might get increased by up to 15% for a HOM-power of 5% and by 20% for a HOM power of 10%. In the majority of cases, however, the HOMs decrease the peak power density.

The results for the truncation losses are shown in Fig. 9. The loss for a pure LP_{01} mode is 0.23 % (see Table 1) and we can see, that this value is almost always increased by HOMs. Only in very few cases, a negative interference of the fields outside of the mirror boundary can result in a reduction of the truncation loss due to HOMs.

The results for the power in the deposition area are shown in Fig. 10. Here the HOMs result mostly in a reduction of the total efficiency. On the other hand the strongest reduction is by about 4.5% for a HOM power of 5% and by 8.5% for a HOM power of 10%. These results indicate that the worst-case estimation proposed in Section II (the relative reduction of the overall efficiency by HOMs is limited by the relative HOM content) is correct.

VI. CONCLUSION

We developed and demonstrated a Monte Carlo method for the estimation of the effects of spurious modes in a hypothetical ECRH launcher. We obtain histograms for the expected values of the truncation loss, the peak power density on the mirror and the overall heating efficiency. Especially the former two are a result of local interference phenomena and can only be assessed statistically. Once this method is applied to a realistic ECRH system, it allows a detailed risk assessment and the definition of safety margins to prevent overheating or arcing.

For the estimation of the power density at sensitive in-vessel components, like diagnostic antennas, our method would be limited to the cases, where the direct exposure to a spurious beam lobe is expected to be the major risk. In general cases, the power density is dominated by isotropic stray radiation, which is modeled with different methods [16].

Even though the presented method was developed with the focus on high power millimeter wave systems, it is generic enough to be applied to many other linear electromagnetic systems, where HOMs can affect the performance. Furthermore, it is completely independent from the simulation methods used to calculate the fundamental solutions, as long as the results are available in terms of complex field vectors.

VII. OUTLOOK

To develop and demonstrate this framework, a very simple generator for mode mixtures (described in Section III) was used. Its main weakness is, that it does not distinguish between the different HOMs, resulting in equivalent distributions (e.g. Fig. 2) for all modes considered. The generation of HOMs, however, has been investigated much more detailed in different studies especially for the ITER transmission line ([7], [17], [18]).

When the method is applied to a real ECRH system, more realistic power levels should be used for the different HOMs based on previous studies. They can still be varied using e.g. a Gaussian distribution for the power and a uniform distribution for the phase. The generation of the mixtures, however, is only a small module in the calculation framework, which can easily be replaced.

REFERENCES

[1] S. P. Morgan, "Mode conversion losses in transmission of circular electric waves through slightly non cylindrical guides," *J. Appl. Phys.*, vol. 21, no. 4, pp. 329–338, 1950, doi: 10.1063/1.1699664.

[2] H. E. Rowe and W. D. Warters, "Transmission in multimode waveguide with random imperfections," *Bell Syst. Tech. J.*, vol. 41, no. 3, pp. 1031–1170, 1962, doi: 10.1002/j.1538-7305.1962.tb00487.x.

[3] J. Doane, "Propagation and mode coupling in corrugated and smooth-wall circular waveguides," in *Infrared and Millimeter Waves*, vol. 13. Orlando, FL, USA: Academic, 1985, pp. 123–170.

[4] H. Li and M. Thumm, "Mode conversion due to curvature in corrugated waveguides," *Int. J. Electron.*, vol. 71, no. 2, pp. 333–347, 1991, doi: 10.1080/00207219108925480.

[5] H. Li and M. Thumm, "Mode coupling in corrugated waveguides with varying wall impedance and diameter change," *Int. J. Electron.*, vol. 71, no. 5, pp. 827–844, 1991, doi: 10.1080/00207219108925527.

[6] J. Doane and C. Moeller, "HE_{11} mitre bends and gaps in a circular corrugated waveguide," *Int. J. Electron.*, vol. 77, no. 4, pp. 489–509, 1994, doi: 10.1080/00207219408926081.

[7] M. C. Kaufman, C. Lau, and G. R. Hanson, "Microwave analysis with Monte Carlo methods for ECH transmission lines," *J. Infrared, Millimeter, THz Waves*, vol. 39, no. 5, pp. 456–482, May 2018, doi: 10.1007/s10762-018-0475-5.

[8] H. Carlin, "The scattering matrix in network theory," *IRE Trans. Circuit Theory*, vol. 3, no. 2, pp. 88–97, 1956, doi: 10.1109/TCT.1956.1086297.

[9] J. Pace, "The generalized scattering matrix analysis of waveguide discontinuity problems," Illinois Univ. Urbana Engineering Experiment Station, Tech. Rep. AD0601131, 1964. [Online]. Available: https://apps.dtic.mil/sti/citations/AD0601131

[10] B. Plaum, "Simulation of microwave beams with PROFUSION (2022 Edition)," Univ. Stuttgart, Tech. Rep., 2022, doi: 10.18419/opus-12241. [Online]. Available: http://elib.uni-stuttgart.de/handle/11682/12258

[11] B. Plaum, M. Preynas, and M. Choe, "Calculations for the optical system for the first ITER plasma," *EPJ Web Conf.*, 2023, vol. 277, Art. no. 01005, doi: 10.1051/epjconf/202327701005.

[12] E. J. Kowalski et al., "Linearly polarized modes of a corrugated metallic waveguide," *IEEE Trans. Microw. Theory Techn.*, vol. 58, no. 11, pp. 2772–2780, Nov. 2010, doi: 10.1109/TMTT.2010.2078972.

[13] J. Murphy, "Distortion of a simple Gaussian beam on reflection from off-axis ellipsoidal mirrors," *Int. J. Infrared Millimeter Waves*, vol. 8, pp. 1165–1187, 1987, doi: 10.1007/BF01010819.

[14] D. Vinogradov, "Mirror conversion of Gaussian beams with simple astigmatism," *Int. J. Infrared Millimeter Waves*, vol. 16, no. 11, pp. 1945–1963, Nov. 1995, doi: 10.1007/BF02072550.

[15] L. Empacher and W. Kasparek, "Analysis of a multiple-beam waveguide for free-space transmission of microwaves," *IEEE Trans. Antennas Propag.*, vol. 49, no. 3, pp. 483–493, Mar. 2001, doi: 10.1109/8.918625.

[16] D. Moseev et al., "Stray radiation energy fluxes in ITER based on a multiresonator model," *Fusion Eng. Des.*, vol. 172, 2021, Art. no. 112754, doi: 10.1016/j.fusengdes.2021.112754.

[17] D. S. Tax et al., "Mode conversion losses in ITER transmission lines," in *Proc. 33rd Int. Conf. Infrared, Millimeter THz Waves*, 2008, pp. 1–2.

[18] M. A. Shapiro et al., "Loss estimate for ITER ECH transmission line," in *Proc. APS Division Plasma Phys. Meeting Abstr.*, 2009, Paper GP8.015.

BURKHARD PLAUM received the Diploma and Doctoral degrees from the University of Stuttgart, Stuttgart, Germany, in 1997 and 2001 respectively. He is a Permanent Staff Member and Lecturer with the Microwave Technology Group of the Institute for Interfacial Process Engineering and Plasma Technology, University of Stuttgart. He works on the design of millimeter wave components and -systems for heating and diagnostic applications in nuclear fusion experiments such as ASDEX upgrade, wendelstein 7-X and ITER.